

Investigation into the Interaction of the Phosphoporin PhoE with Outer Membrane Lipids: Physicochemical Characterization and Biological Activity

Jörg Andrä¹, Hans de Cock², Patrick Garidel³, Jörg Howe¹ and Klaus Brandenburg^{*,1}

¹Forschungszentrum Borstel, Leibniz-Zentrum für Medizin und Biowissenschaften, D-23845 Borstel, Germany;

²Universiteit Utrecht, Institute of Biomembranes, Utrecht, The Netherlands; ³Martin-Luther Universität Halle-Wittenberg, Institut für Physikalische Chemie, D-06108 Halle, Germany

Abstract: Outer membrane pore proteins such as phosphoporin (PhoE) are important constituents of Gram-negative bacteria such as *Escherichia coli*. We have studied the interaction of PhoE with the membrane-forming lipids phosphatidylethanolamine (PE) and phosphatidylglycerol (PG) from the inner and lipopolysaccharide (LPS) from the outer leaflet of the outer membrane. These investigations comprise functional aspects of the protein:lipid interaction corresponding to the outer membrane system as well as the activity of LPS:PhoE complexes in the infected host after release from the bacterial surface. The interaction of the lipids PE, PG, and LPS with PhoE was investigated by analysing molecular groups in the lipids originating from the apolar region (methylene groups), the interface groups (ester), and polar groups (phosphates) applying Fourier-transform infrared spectroscopy (FTIR), and by analysing the phase transition behaviour of the lipids using FTIR and differential scanning calorimetry (DSC). The activity of PhoE and LPS:PhoE complexes was investigated in biological test systems (human mononuclear cells and *Limulus* amoebocyte lysate assay) and with phospholipid model membranes using fluorescence resonance energy transfer spectroscopy (FRET). The results show a strong influence of PhoE on the mobility of the lipids leading to a considerable fluidization of the acyl chains of LPS, but much less to those from phospholipids: PhoE released from the outer membrane still contains slight contaminations of LPS, but its strong cytokine-inducing ability in mononuclear cells, which is not found in the LPS-specific *Limulus* amoebocyte lysate test, indicates an LPS-independent mechanism of cell activation.

Key Words: PhoE, LPS, cytokine induction, membrane fluidity, outer membrane.

INTRODUCTION

Outer membrane proteins PhoE, 36.8 kDa phosphoporins, are assembled as trimers in the outer membrane (OM). PhoE has strong sequence-similarity as well as in the general structure with porins OmpF and OmpC [1]. It is specific for anions, but has no specificity for phosphates. It was shown in former studies that the chemical structure and biophysical properties of LPS are important for a correct and efficient folding of PhoE into the outer membrane [2].

Generally, for the proper function of Omp's the properties of the matrix lipids embedding the latter are of importance as has been shown previously for porins [3]. A mixture of phosphatidylethanolamine (PE), phosphatidylglycerol (PG), and cardiolipin in a molar ratio of 87:12:1 forms the inner leaflet of the outer membrane, whereas lipopolysaccharide (LPS) is the exclusive lipid of the outer leaflet, i.e., the outer membrane is strongly asymmetric [4]. It was found that the intercalation of the porins OmpC and OmpF from the cytoplasmic side of the membrane – similar to the situation *in vivo* – strongly depends on the presence of LPS on the opposing side [3].

During infection, components of the bacterial membranes are released into the environment due to the attack of the immune system or simply due to cell division. Since it is known that in particular membrane proteins and LPS form complexes, it can be assumed that these play a significant role also in the host, for example by interacting with immune cells such as human mononuclear cells leading to cell activation and induction of cytokines. It has been shown that LPS alone elicits a variety of biological reactions in mammals ranging from beneficial to pathological ones such as the septic shock syndrome [5]. Thus, LPS is known to be one of the most potent stimuli of the immune system. Furthermore, it was found that also porins may stimulate cytokines such as interleukins and tumor-necrosis-factor α [6-10].

In a recent paper, we have characterized the interaction of the outer membrane protease OmpT with outer membrane lipids and have found specific protein:lipid interactions differing for the lipids, phospholipids and LPS [6]. Furthermore, OmpT by itself led to activation of immune cells.

In the present paper, the interaction of PhoE with membrane phospholipids and LPS – essential for its function in the bacterial outer membrane – is studied with infrared spectroscopy by investigating the (i) influence of the proteins on the gel to liquid crystalline phase behaviour of the lipids – supplemented by differential scanning calorimetric (DSC) experiments, and on the phosphate band contour of the lipids, and (ii) the influence of the lipids on the secondary

*Address correspondence to this author at the Forschungszentrum Borstel, Leibniz-Institut für Medizin und Biowissenschaften, Div. of Biophysics, Parkallee 10, D-23845 Borstel, Germany; Tel: +49-(0)4537-188235; Fax: +49-(0)4537-188632; E-mail: Kbranden@fz-borstel.de

structure of the protein. Furthermore, the interaction of pure PhoE or LPS:PhoE complexes with phospholipid target cell membranes was studied with fluorescence resonance energy transfer spectroscopy (FRET). In biological assays, the ability of PhoE alone and in the presence of LPS to induce an inflammatory response (cytokine induction in human mononuclear cells) or a coagulation reaction (*Limulus* ameobocyte lysate assay) was tested.

RESULTS

Gel to Liquid Crystalline Phase Transition

In the following, the acyl chain melting induced by PhoE was studied for natural phosphatidylethanolamine (PE) and phosphatidylglycerol (PG) and for deep rough mutant LPS Re from *Salmonella minnesota* strain R595. The gel (β) to liquid crystalline (α) phase transition of the hydrocarbon chains was monitored by analysing the peak position of the symmetric stretching vibrational band $\nu_s(\text{CH}_2)$ as a function of temperature. The results in Fig. 1 given for the two phospholipids (a,b) and LPS (c) exhibit – except for PG in the liquid crystalline phase – a distinct fluidization of the acyl chains and a decrease of the phase transition temperature T_c for all lipids due to the presence of PhoE. This can be taken from the increase of the wavenumber values at a given temperature. The effects occur already at very low PhoE concentrations, in particular for LPS already at [LPS]:[PhoE] = 1200:1 molar. At 37 °C, for PE and LPS, but not for the PG preparation the wavenumbers increase significantly.

Supplementary to the IR measurements also differential scanning calorimetry (DSC) was applied to the [LPS Re]:[PhoE] system (Fig. 2). The thermodynamic data of pure LPS for the phase transition from a gel to the liquid crystalline phase are: phase transition temperature $T_c = \sim 31$ °C ($T_{1/2} = 4.5$ °C) with a phase transition enthalpy of $\Delta H_c = 39$ kJ/mol. As can be seen from the FTIR results, PhoE induces a strong destabilisation of the gel phase of LPS and as a consequence the phase transition temperature is shifted to lower temperature as found for LPS above. Even in the presence of very small amounts of PhoE e.g. at a molar ratio of [LPS]:[PhoE] 250:1, it induces a destabilisation of the gel phase and a reduction of the phase transition enthalpy of ~ 12 %. Additionally, a strong broadening of the low temperature side of the heat capacity curve, is observed. At a LPS to PhoE molar ratio of 62:1 $T_c = 30.6$ °C with $\Delta H_c \sim 25$ kJ/mol.

The cooling-scans of the system [LPS]:[PhoE] are represented by a sharp exothermic peak between 33–34 °C with a large tailing on the low temperature side of the heat capacity curve, which has been described previously (data not shown, [6]). The second heating-scan shows a broad thermogram with a peak maximum shifted around ~ 35 °C indicating a stabilisation of the gel phase. However, the 2nd heating-scan represents the interaction of LPS liposomes with denaturated protein, due to the fact that in the 1st scan heating was performed to 95 °C: Thus, the first heating scan represents the lipid interaction with the native protein, leading to a destabilisation of the gel phase transition.

Binding of PhoE to LPS membranes provokes a strong perturbation of the organisation of the lipid hydrocarbon chains. The broadening of the low temperature side of the

heat capacity curve as well as a decrease of the phase transition enthalpy is indicative for the reduction of the van der Waals interactions between the lipid acyl chains leading to increased hydrocarbon chain fluidity of the gel phase.

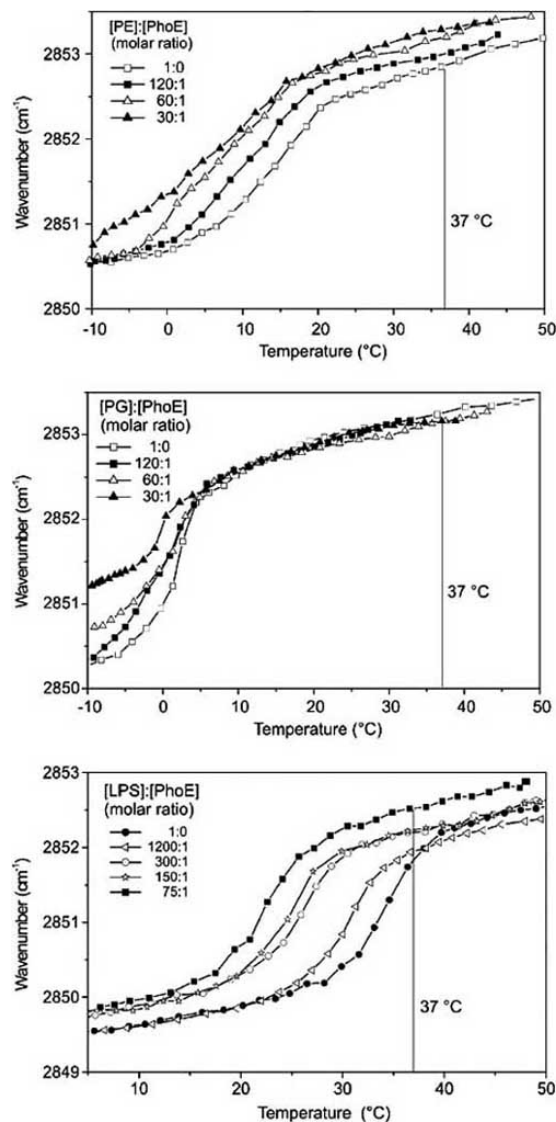


Fig. (1). Peak position of the symmetric stretching vibrational band $\nu_s(\text{CH}_2)$ versus temperature for different molar [PE]:[PhoE] (a), [PG]:[PhoE] (b), and [LPS]:[PhoE] (c) ratios. In the gel (α) phase of the acyl chains, the typical peak position is around 2849.5 to 2850.5 cm^{-1} , in the liquid crystalline (β) phase it is located in the range 2852.5 to 2854 cm^{-1} .

Phosphate Band Contour of the Lipids

Infrared spectra were analysed in the wavenumber range 1280 to 1140 cm^{-1} consisting of vibrational bands typical for the antisymmetric stretch of the negatively charged phosphate $\nu_{as}(\text{PO}_2^-)$ between 1200 and 1260 cm^{-1} , for the single ester bond (C-O) around 1180 cm^{-1} , and in the case of LPS, the diglucosamine ring vibration in the range 1160 to 1180 cm^{-1} .

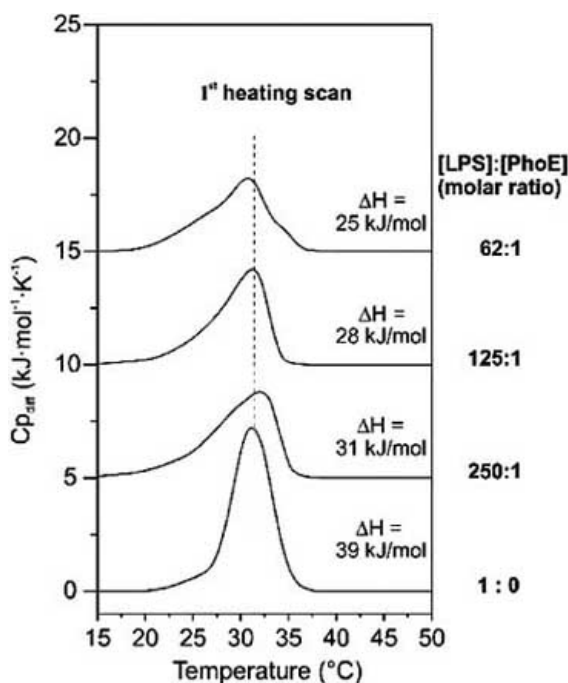


Fig. (2). Differential calorimetric scans of LPS Re (1 mg/ml) with varying concentrations of PhoE. The molar ratios are indicated at the right margin, and also the enthalpy changes corresponding to the areas of the endothermic transitions.

Additionally, for gel phase lipids also wagging progression bands may be present in this spectral range, which, however, can be neglected here, since the measurements were performed above T_c . For LPS at least two phosphate band components in the range 1200 to 1280 cm^{-1} can be observed (Fig. 3c) due to the existence of differently hydrated phosphate groups with the component at the higher wavenumber corresponding to a more dehydrated state (described for the system PG: Mg^{2+} by Garidel *et al.* [7]). For the phospholipids, the main bands around 1220 cm^{-1} are significantly suppressed for PE in the presence of PhoE (Fig. 3a), whereas for PG (Fig. 3b) only minor changes are observed. For LPS, increasing concentrations of PhoE lead to an intensity decrease particular of the band component around 1220 cm^{-1} , as well as of the diglucosamine band. This is indicative of an interaction of PhoE especially with the diglucosamine -1-phosphate region of the lipid A backbone, since it has been shown that in this backbone the 1-phosphate is highly and the 4'-phosphate only low hydrated [8]. Summarized, a strong interaction of PhoE with the phosphate region of LPS and PE, but not of PG is observed.

Secondary Structure of PhoE

The analysis of the secondary structure of PhoE in the absence and presence of the different lipids was done by evaluating the IR spectrum in the range of the amide I-vibrational band, which shows a complex splitting into single components according to the water binding capability of the secondary structures [9]. The characteristic secondary structures for α -helical structures are in the range 1650 to

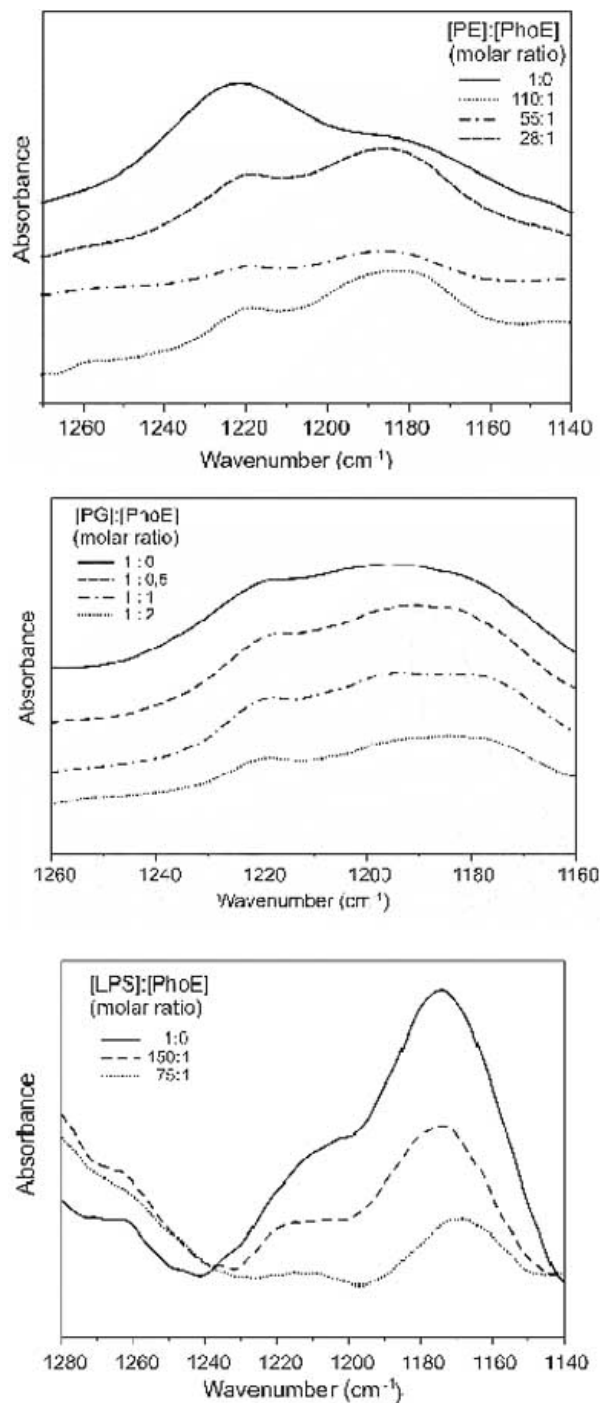


Fig. (3). Infrared spectra in the wavenumber region characteristic for the phosphate band contour for [PE]:[PhoE] (a), [PG]:[PhoE] (b), and [LPS]:[PhoE] (c) mixtures above the respective phase transitions T_c . The band components in the lower wavenumber range (1210 to 1240 cm^{-1}) correspond to highly hydrated, those in the higher wavenumber range (1240 to 1270 cm^{-1}) to less hydrated phosphate groups. The band component around 1180 cm^{-1} results for the phospholipids mainly from the ester single stretch $\nu(\text{C-O})$ and for LPS from a diglucosamine vibration.

1658 cm^{-1} , the main peaks for β -sheet structures are in the range 1628 to 1635 cm^{-1} , and other bands may lie around 1620 cm^{-1} corresponding to intermolecular aggregated forms, and around 1670 to 1685 cm^{-1} for β -turns and antiparallel β -sheets, respectively. Random coil (unordered) structures lie in the range 1658 to 1665 cm^{-1} , which are shifted to 1640 – 1645 cm^{-1} if D_2O instead of H_2O is used in the buffer. We have measured in both solutes to avoid a possible misinterpretation of the α -helical and unordered structures. Fig. 4 (A) shows the infrared spectrum of hydrated (H_2O) PhoE in the amide I-region, which indicate the occurrence of β -sheet as well as α -helical structures, and further β -type structures (turns, intermolecular sheets).

The corresponding spectra in the presence of the lipids in Fig. 4 shows clearly a dramatic increase of the amount of β -sheet structures of the protein (band around 1630 cm^{-1}) in the presence of the negatively charged lipids PG and LPS (C,D), whereas PE (B) leads to an only very small change of the secondary structures of PhoE.

It should be noted that the measurements in D_2O lead to very similar results, in particular, the α -helical structures cannot be misinterpreted as resulting from unordered structures. Furthermore, as control PhoE was boiled for 1

hour, which should destroy the highly ordered α -structures, and was actually found to be true (data not shown).

Incorporation into Target Membranes

To test the possibility that PhoE as membrane protein could not only be able to intercalate into bacterial outer membranes, but also into membranes of host cells such as the macrophages, we have applied FRET spectroscopy. In Fig. 5, the results are shown for negatively charged phosphatidylserine liposomes. No signal is observed for the buffer control, a very slight increase of the FRET signal for the control protein OmpT, and a considerable increase for LPS-free PhoE. Similar results were obtained when the phospholipid liposomes were prepared according to the composition of macrophage membranes. In particular, no incorporation was observed for OmpT in accordance to our former study [6].

Biological Activity

Outer membrane components like LPS are known to stimulate macrophages. When proteins such as PhoE are released from the outer membrane for example by the influence of the immune system, they are generally regarded as complexed with LPS and as such may be active to

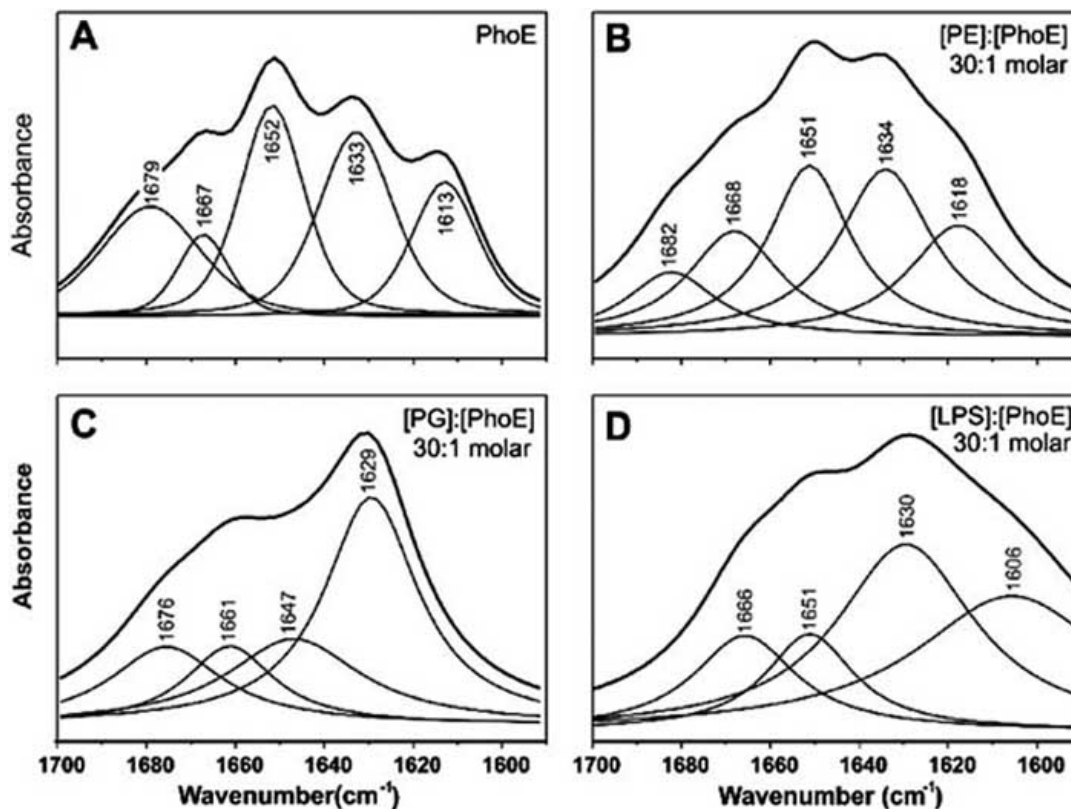


Fig. (4). Infrared spectra in the range 1700 to 1590 cm^{-1} characteristic for the amide I vibrational band (predominantly C=O) for pure PhoE (a) and for PE- (b), PG- (c), and LPS- (d) PhoE mixtures at [lipid]:[PhoE] = 30:1 molar. The main band component around 1625 to 1640 cm^{-1} is characteristic for β -sheet, that around 1650 to 1660 cm^{-1} for α -helical structures [9]. Further band components around 1610 to 1620 cm^{-1} correspond to intermolecular aggregates and around 1670 to 1685 cm^{-1} to β -turns and antiparallel β -sheets.

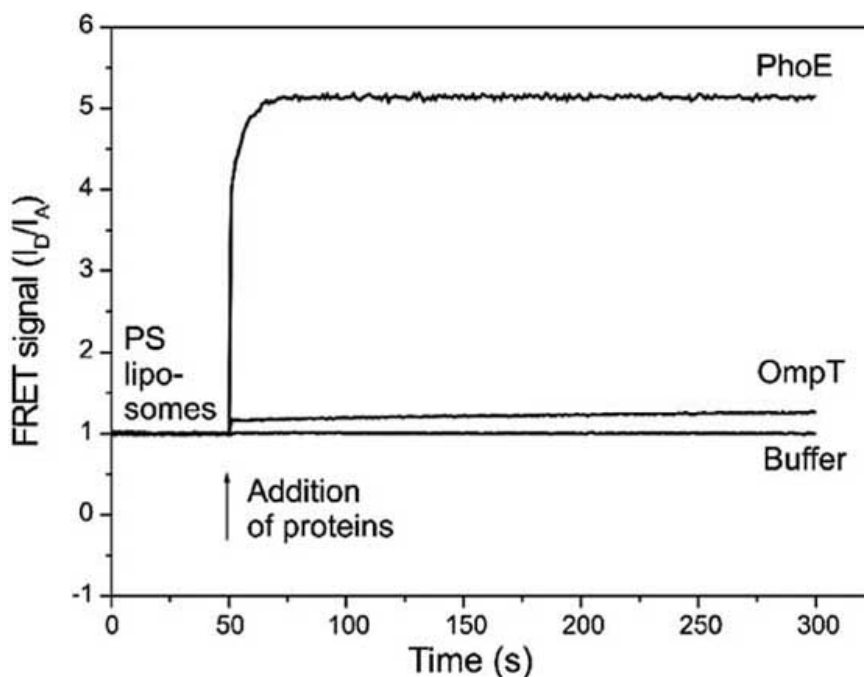


Fig. (5). Time dependence of the ratio of fluorescence intensity I_D at 531 nm to that of the acceptor fluorescence intensity at 593 nm (FRET signal) for PhoE in comparison to the protein OmpT and buffer.

stimulate macrophages. However, membrane proteins such as porins may exert biological activity directly by themselves, thus independent of LPS to which they are complexed [6-10]. We have therefore investigated the ability of LPS-free PhoE as well as [LPS]:[PhoE] mixtures in comparison to LPS (i) to induce the production of tumor-necrosis-factor α (TNF α) in human mononuclear cells (MNC) and (ii) to react in the *Limulus* amoebocyte lysate (LAL) assay.

In Fig. 6, the TNF α -production of human MNC induced by different concentrations of PhoE and LPS:PhoE mixtures is shown. Clearly, LPS has a very high cytokine-producing ability at all investigated concentrations (left-hand bars). Interestingly, the addition of excess PhoE on a weight basis causes a reduction of immunostimulatory activity (bars in the middle), and LPS-free PhoE induced significant amounts of the cytokine (bars on the right-hand side). The sum of the cytokine production values of each the pure LPS and PhoE is much higher than those found for the LPS-PhoE mixtures, from which a complexation of the LPS:PhoE mixture different from a pure adsorption can be deduced.

The PhoE protein used has been obtained by refolding of PhoE that was purified from inclusion bodies and refolded in the absence of LPS and is therefore regarded LPS-free. Nevertheless, to test a possible contamination of PhoE with LPS, the *Limulus* amoebocyte lysate assay (LAL) was applied, which is specific for LPS and does not react with proteins. As presented in Fig. 7, the reactivity for PhoE (1.7 EU/ml) is indeed extremely low and is indicative of virtual absence of LPS. Also, the results for the boiled PhoE, which should lead to a denaturation of the protein, but should not

influence LPS bioactivity, are indicative that only sporadic amounts of LPS can be present in the PhoE preparation.

DISCUSSION

The study of the interaction of PhoE with the outer membrane constituents PE, PG, and LPS clearly prove a tight binding of the protein with the main lipid compounds PE and LPS (Fig. 1-3). This interaction leads to a fluidization of the acyl chains of the lipids (Fig. 1a,c). For PG, however, there is only a slight fluidization below T_c far below the physiological temperature (Fig. 1b). Regarding the fact that LPS and PE are the main components of the outer membrane - the PG content of the inner leaflet of the outer membrane is less than 20 % of the lipids [10] - it can be assumed that the presence of PhoE reduces the acyl chain order also within the asymmetric bilayer of the outer membrane. This fluidization starts already at a very low PhoE:lipid molar ratio and can thus be assumed to be physiologically relevant.

The absence of a specific interaction of PhoE with PG becomes also evident from the phosphate vibration (Fig. 3b), the band intensity of which is strongest reduced for PE (Fig. 3a), less for LPS (Fig. 3c), but is not influenced by the presence of PG.

In accordance with the 'high state of order of LPS' [11] it has been published that the outer membrane represents a high permeability barrier in particular against large hydrophobic drugs due to the existence of the LPS outer leaflet, in particular the highly ordered hydrocarbon moiety [12-13]. These properties may hold truth for the pure lipid matrix. Our data obtained in the presence of PhoE and this is

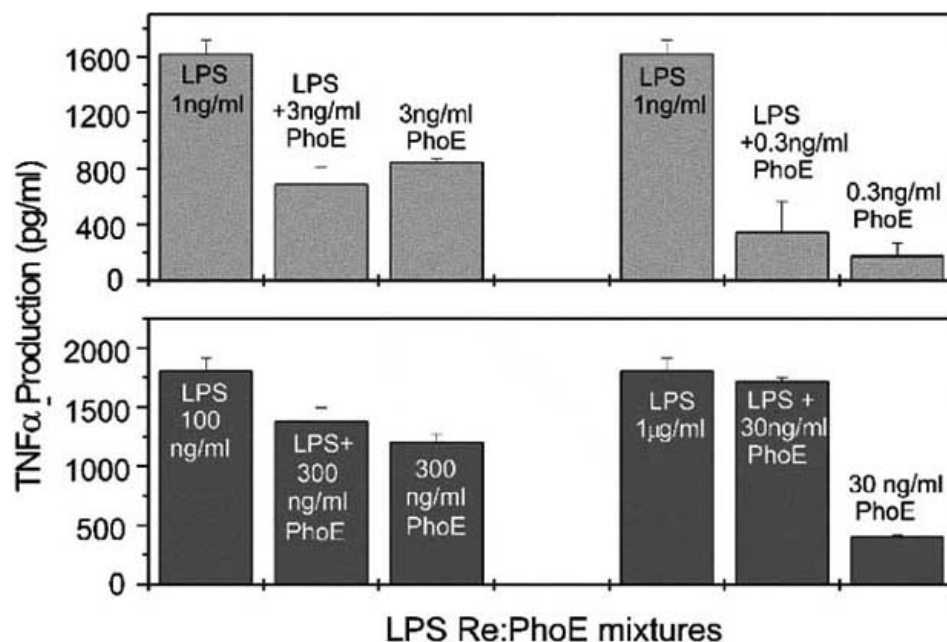


Fig. (6). Production of tumor-necrosis-factor- α (TNF α) by human mononuclear cells induced by different concentrations of LPS, LPS:PhoE-mixtures, and PhoE. The error bars (standard deviation) result from the determination of TNF α in duplicate at two different dilutions. The data are representative of three independent experiments.

in accordance to recent results published for OmpT [6], however, do not indicate a significantly higher order of the LPS as compared to that of the phospholipids. Regarding the barrier property, it seems to be much more probable that the extremely hydrophilic sugar headgroup of LPS is responsible for this. Thus, this can be enhanced by cation bridging between neighbouring molecules *via* the negative charges in the LPS backbone and/or those in the core oligosaccharide [14], leading to a tight network of sugar chains with a strong water-binding capacity. Therefore, one main role of integral membrane proteins such as PhoE and OmpT seems to level the existing acyl chain mobility gradients between the two leaflets of the outer membrane, since, as can be seen in Fig. 1a-c, the wavenumber values at 37 °C for all three lipids approach more and more with increasing PhoE concentrations.

Both the IR spectroscopic data (Fig. 1) and the DSC data (Fig. 2) indicate a gel phase destabilisation of LPS by integral OMP's like PhoE and OmpT, connected with a decrease of the lipid T_c and a considerable reduction in the phase transition enthalpy change. This is in contrast to what has been described previously for the interaction of LPS with non-integral proteins like lysozyme [15] and lactoferrin [16], haemoglobin from red blood cells [17], high-density lipoprotein HDL [18] and (recombinant) albumin [19]. All these non-membrane proteins exhibit a gel phase stabilization, connected with an increase in T_c . Thus, this basic difference may reflect complete different functions of the various proteins. Very importantly, the strong fluidization of the LPS acyl chains is not a singular property of PhoE and OmpT; we have found that also the porins from the bacterial outer membrane induce a similar effect already at very low protein

concentrations (own unpublished data in collaboration with W. Welte, Universität Konstanz).

The fluidizing role of PhoE seems also to be important with respect to the outer membrane stability. The phase transition temperature T_c of pure enterobacterial LPS was found to lie close to the physiological temperature (see Fig. 2), in particular for various smooth form LPS even at temperatures > 37 °C [20]. Interestingly, it has been experimentally verified with a planar asymmetric membrane system (Hagge *et al.*, Forschungszentrum Borstel, unpublished results) that such membranes are too unstable due to the high rigidity of the acyl chains.

Noteworthy are the data from the secondary structure determination of PhoE (Fig. 6 and Table 2), and emphasize the importance of the water content on the interpretation of the spectra. Cowan *et al.*, [1] have elucidated the crystal structure of PhoE and found, that the channel-forming motif was a 16-strand anti-parallel β -barrel. These data seem to be in contradiction to the presented data (Fig. 4), which indicate a considerable contribution of α -helical structures.

To understand this contradiction, it has to be considered that the presence of a relatively high water content as applied here may play a role. For example, 'solution' structure of the protein α -lactalbumin deduced from CD and FTIR spectroscopy dramatically differed from the crystal structure as determined by X-ray crystallography [21]. The solution structure had much less helical (α - and 3_{10} -) structures than the protein crystal. Furthermore, the fact that the addition of negatively charged lipids (PG, LPS) lead to the strong enhancement of β - at the expense of α -structures (Fig. 4C,D), may be indicative that in the crystallographic

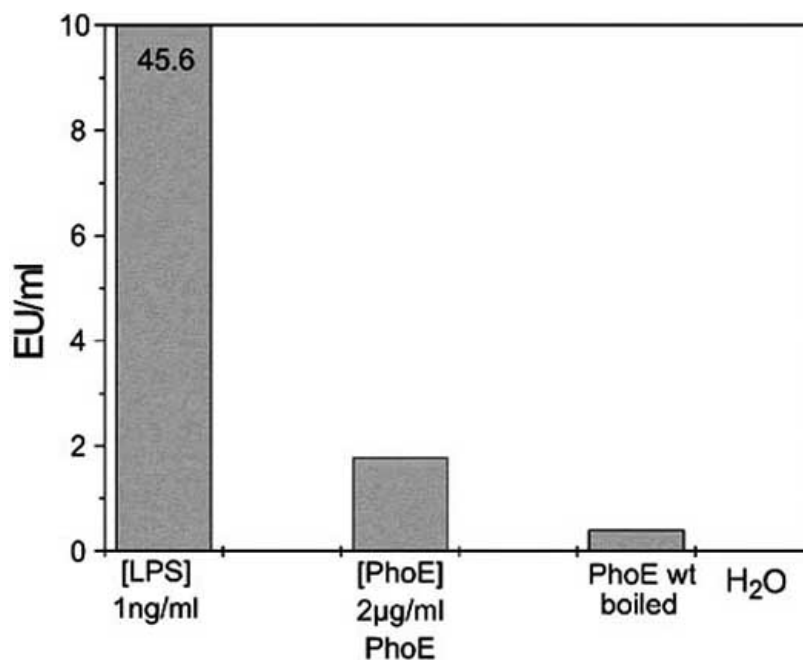


Fig. (7). Endotoxin activity in the *Limulus* amoebocyte lysate assay (in Endotoxin units/ml) of LPS, PhoE, and boiled PhoE as compared to pure water. The figure is a representative result of three different determinations.

experiments the protein was not free of PG and/or LPS. Alternatively or in addition, the interaction of the lipids with refolded and near-native PhoE triggered some final steps in folding with concomitant increase in β -content.

The data of the cytokine induction in human mononuclear cells induced by LPS, PhoE and LPS:PhoE mixtures (Fig. 6) indicate a strong capacity of the protein to induce TNF α production. This is not due to contamination of PhoE with LPS since only sporadic amounts of LPS might be present - considering the results from the experiments with the protein in the *Limulus* assay (Fig. 7) - as to explain this potency. Furthermore, the addition of corresponding concentrations of LPS leading by itself to a high signal even reduces the TNF α inducing capacity of pure PhoE (see Fig. 6, top). Interesting are the results for the mixtures: the addition of PhoE to LPS Re at the given concentrations in all cases lead to a decrease in LPS Re immunostimulatory activity, which might be explained by the fact that the binding sites in LPS Re for serum- and membrane proteins such as LBP and CD14 are partially hidden or occupied. Concomitantly, or as an alternative model, it is also possible that the LPS aggregate structure is stabilized by binding to PhoE which would increase the binding energy of the LPS molecules within the aggregate. This would run parallel to the action of the polycationic decapeptide polymyxin B (PMB), which also leads to a strong fluidization of the lipid A acyl chains of LPS [22] and an increase in the binding energy for lipid A aggregates from -490 meV to more than -570 meV [23].

The capacity of PhoE to induce cytokines such as TNF α in mononuclear cells can be assumed to result from an

incorporation of the protein into the membrane of these cells, since the FRET data (Fig. 5) show a corresponding signal. It has never been reported that PhoE proteins may induce cytokines. However, the data in our previous report on OmpT [6] and other literature data indicate the ability of membrane proteins for cell activation.

The group of Galdiero [24] was the first who described cytokine induction in human monocytes. They studied the release of TNF α , IL-1, and IL-6 by human monocytes and of γ -interferon and IL-4 by lymphocytes, induced by porins from rough mutant and wild-type strains from *Salmonella typhimurium*. Analogously, others [25] studied the immunomodulatory properties of some porins from Enterobacteria and found, among others, an IL-1 induction in peritoneal cells from mice. In a more detailed study Galdiero and co-workers [26] found cytokine (IL-6, IL-8, and TNF α) induction in the human monocyte cell line THP-1 already at a porin concentration of 50 ng/ml. Furthermore, neither the presence of serum nor CD14 influenced this activity, only the presence of the integrins CD11a/CD18 exhibited a slight influence. Investigations into the early responses after porin stimulation showed that the cell signalling pathways include activating protein 1 (AP1) and nuclear factor κ B (NF- κ B) through the mitogen-activated protein kinase (MAPK) cascade [27]. The authors found differences to the signalling by LPS, because the cytokine release after stimulation with porins began after 2 hours and lasted for 5 to 6 h, whereas that after LPS stimulation started after 30 min and decreased after 2 hours. The authors also tested the porin preparations for a LPS contamination by applying the *Limulus* test as well as polymyxin B to remove LPS, but found no evidence for a

contamination. Massari *et al.*, [28] found stimulation of murine B cells by *Neisseria* porins to be dependent on TLR2 and the adapter protein MyD88, which was deduced from the lack of response in TLR2- and MyD88- knockout mice.

EXPERIMENTAL

Lipids and Reagents

Lipopolysaccharide from the Re mutant of *Salmonella minnesota* (R595) were extracted by the phenol/chloroform/petrol ether method [29] from bacteria grown at 37 °C, purified, and lyophilized. Bovine brain phosphatidylserine, egg phosphatidylcholine, phosphatidylethanolamine (PE) and phosphatidylglycerol (PG) from *E. coli*, and sphingomyelin from bovine brain were purchased from Avanti Polar Lipids (Alabaster, AL, USA).

PhoE

The mature form of PhoE protein was expressed and isolated from *Escheichia coli* strain BL21(DE3) cells containing plasmid pCJ2 and refolded into a trypsin-resistant form with high amounts of SDS and heat-stable trimers [30] as described previously [31]. PhoE was diluted in aqueous solution containing 0.15 mg/ml Triton X-100 and stored at 4 °C for at least 3 days before use.

Sample Preparation

The lipid samples were usually prepared as aqueous dispersions (1 to 10 mM) for the phase transition measurements (FTIR, DSC) or as hydrated samples for the other infrared spectra. The latter spectra were recorded at the instrument temperature of 28 °C. The lipids were prepared by suspending them directly in HEPES buffer, sonicating and temperature-cycling for several times between 5 and 70 °C and then storing at 4 °C for at least 12 h before measurement. For the elucidation of the protein secondary structure in the absence and presence of the lipids, PhoE was prepared in buffer made either from H₂O or D₂O incubated at 37 °C for 0.5 h, and lipid dispersions prepared as described above were added in appropriate amounts, and further incubated at 37 °C for 15 min. Afterwards, 10 µl of these dispersions were spread on a CaF₂ infrared window, and the excess water was evaporated slowly at 37 °C.

For preparation of liposomes from a phospholipid mixture corresponding the composition of the cell membrane of macrophages – phosphatidylcholine, phosphatidylserine, phosphatidylethanolamine, and sphingomyelin in a molar ratio of 1:0.4:0.7:0.5 [32], the lipids were solubilized in chloroform, the solvent was evaporated under a stream of nitrogen, lipids were resuspended in the appropriate volume of buffer, and further treated as described for the lipids above.

For the analysis of the secondary structure of the protein *via* the analysis of the amide I band (predominantly C=O stretch) contour, aqueous protein solution were dispersed on a Ge crystal, and the excess water was slowly evaporated by standing at room temperature. The sample was then placed in a closed cuvette and the air above the sample was saturated with water vapour.

FTIR Spectroscopy

The infrared spectroscopic measurements were performed on a IFS-55 spectrometer (Bruker, Karlsruhe, Germany). For the phase transition measurements *via* the analysis of the peak position of the symmetric stretching vibrational band of the methylene group at 2850 cm⁻¹, the lipid samples were placed in a CaF₂ cuvette with a 12.5 µm teflon spacer. Temperature-scans were performed automatically between 10 and 70 °C with a heating-rate of 0.6 °C/min. Every 3 °C, 50 interferograms were accumulated, apodized, Fourier transformed, and converted to absorbance spectra.

For strong absorption bands, the band parameters (peak position, band width, and intensity) were evaluated from the original spectra, if necessary after subtraction of the intensive water bands. The position of the peak maxima was determined with a precision of better than 0.1 cm⁻¹. The infrared spectra were evaluated after base-line subtraction of neighboring bands. In the case of overlapping bands, in particular for the analysis of the amide I-vibration, curve fitting was applied using a modified version of the CURFIT program obtained by D. Moffat, NRC, Ottawa, Canada. An estimate of the number of band components was obtained from deconvolution of the spectra [33], and the curve was fitted to the original spectra after subtraction of base-lines resulting from neighboring bands. The bandshapes of the single components are superpositions of Gaussian and Lorentzian. Best fits were obtained by assuming a Gauss fraction of 0.55- 0.60.

Differential Scanning Calorimetry (DSC)

A stock solution of 1 mg/ml of LPS Re was dispersed in 5 mM phosphate buffer at pH 6.8. LPS aggregates were obtained by sonication as described previously [19, 22]. A known amount of protein was added to the lipid dispersion at room temperature and the mixture slightly vortexed until full protein dissolution. DSC measurements were performed with a MicroCal VP scanning calorimeter (MicroCal, Inc., Northampton, MA, USA) at heating and cooling rates of 1° C/min. Heating and cooling curves were measured in the temperature interval from 10 to 95 °C. Three consecutive heating and cooling scans were measured. For more details see Blume and Garidel [34].

Fluorescence Resonance Energy Transfer (FRET) Spectroscopy

The FRET assay was performed as described earlier [35, 36]. Briefly, phospholipid liposomes corresponding to the composition of the macrophage membrane (PL_{Mφ}) or from phosphatidylserine were doubly labeled with the fluorescent dyes N-(7-nitrobenz-2-oxa-1,3-diazol-4-yl)-phosphatidylethanolamine (NBD-PE) and N-(lissamine rhodamine B sulfonyl)-phosphatidylethanolamine (Rh-PE) (Molecular Probes, Eugene, OR, USA). Intercalation of unlabeled molecules into the doubly labeled liposomes leads to probe dilution and with that to a lower FRET efficiency: the emission intensity of the donor at 531 nm increase and that of the acceptor at 593 nm decreases. Thus, as sensitive measure of an intercalation the ratio of donor to acceptor intensity I_D/I_A was taken (FRET signal).

In all experiments, the protein PhoE was added after 50 s to the doubly labeled liposomes, and the FRET signal was monitored for at least 300 s.

Stimulation of Human Mononuclear Cells (MNC)

For an examination of the cytokine-inducing capacity of the PhoE and [LPS]:[PhoE] mixtures, human mononuclear cells were stimulated with these and the TNF α production of the cells was determined in the supernatant.

MNC were isolated from heparinized (20 IE/ml) blood taken from healthy donors and processed directly by mixing with an equal volume of Hank's balanced solution and centrifugation on a Ficoll density gradient for 40 min (21 °C, 500 g). The interphase layer of mononuclear cells was collected and washed twice in Hank's medium and once in RPMI 1640 containing 2 mM L-glutamine, 100 U/ml penicillin, and 100 μ g/ml streptomycin. The cells were resuspended in medium and the cell number was equilibrated at 5×10^6 N/ml. For stimulation, 200 μ l/well MNC (5×10^6 cells/ml) were transferred into 96-well culture plates. The stimuli were serially diluted in serum-free RPMI 1640 and added to the cultures at 20 μ l per well. The cultures were incubated for 4 h at 37 °C under 5% CO₂. Cell-free supernatants were collected after centrifugation of the culture plates for 10 min at 400 g and stored at -20 °C until determination of cytokine content.

Immunological determination of TNF α in the cell supernatant was performed in a sandwich-ELISA as described elsewhere [37]. 96-well plates (Greiner, Solingen, Germany) were coated with a monoclonal (mouse) anti-human TNF α antibody (clone 16 from Intex AG, Switzerland). Cell culture supernatants and the standard (recombinant human TNF α , Intex) were diluted with buffer. After exposure to appropriately diluted test samples and serial dilutions of standard rTNF α , the plates were exposed to peroxidase conjugated (sheep) anti-mouse IgG antibody. Subsequently, the color reaction was started by addition of tetramethylbenzidine/H₂O₂ in alcoholic solution and stopped after 5 to 15 min by addition of 1N sulfuric acid. In the color reaction, the substrate is cleaved enzymatically, and the product was measured photometrically on an ELISA plate reader at a wavelength of 450 nm and the values were related to the standard. TNF α was determined in duplicate at two different dilutions and the values were averaged.

Determination of Endotoxin Activity by the Chromogenic Limulus Test

The biological activity of PhoE and LPS at concentrations between 10 pg/ml and 10 μ g/ml was determined also by using a quantitative kinetic assay based on the reactivity of Gram-negative endotoxin with *Limulus* amoebocyte lysate (LAL) [38], using test kits from LAL Coamatic Chromo-LAL K (Chromogenix, Haemochrom). The standard endotoxin used in this test was from *E. coli* (O113:H10), (EU/ml corresponds to 1 ng/ml). In this assay, saturation occurs at 125 endotoxin units EU/ml, and the resolution limit is ≤ 0.2 EU/ml (maximum value for ultrapure water from Sigma).

ACKNOWLEDGEMENT

We are indebted to G. von Busse and C. Hamann, for performing the IR spectroscopic and fluorescence spectroscopic measurements. The expert help of B. Fölting for performing the DSC and U. Diemer the LAL measurements, respectively, are kindly acknowledged. This work was financially supported by the Commission of the European Communities, specific RTD programme "Quality of Life and Management of Living Resources", QLK-CT-2002-01001", 'Antimicrobial endotoxin neutralizing peptides to combat infectious diseases'.

REFERENCES

- [1] Cowan, S.W.; Schirmer, T.; Rummel, G.; Steiert, M.; Ghosh, R.; Paupit, R.A.; Jansson, J.N.; Rosenbusch, J.P. *Nature*, **1992**, 358, 727.
- [2] De Cock, H.; Brandenburg, K.; Wiese, A.; Holst, O.; Seydel, U. *J.Biol.Chem.*, **1999**, 274, 5114.
- [3] Wiese, A.; Schröder, G.; Brandenburg, K.; Hirsch, A.; Welte, W.; Seydel, U. *Biochim. Biophys. Acta*, **1994**, 1190, 231.
- [4] Nikaido, H.; Vaara, M. in *Escherichia coli and Salmonella typhimurium. Cellular and Molecular Biology*, Neidhardt, Ingraham, Brooks Low, Magasanik, Schaechter, and Umberger. Eds. American Society for Microbiology, Washington, DC **1987**, pp. 7-22.
- [5] Seydel, U.; Ulmer, A.J.; Uhlig, S.; Rietschel, E. Th., in *Membrane Structure in Disease and Drug Therapy*, Zimmer Ed. Marcel Dekker Inc.; New York, **1999**.
- [6] Brandenburg, K.; Garidel, P.; Schromm, A.B.; Andra, J.; Kramer, A.; Egmond, M.; Wiese, A. *Eur. Biophys. J.*, **2005** (in press).
- [7] Garidel, P.; Blume, A. *Biophys. Biochem. Acta*, **2000**, 1466, 245.
- [8] Brandenburg, K.; Kusumoto, S.; Seydel, U. *Biochim. Biophys. Acta*, **1997**, 1329, 193.
- [9] Arrondo, J.L. and Goni, F.M. *Prog. Biophys. Molec. Biol.*, **1999**, 72, 367.
- [10] Osborn, M.J.; Gander, J.E.; Parisi, E.; Carson, J. *J. Biol. Chem.*, **1972**, 247, 3962.
- [11] Labischinski, H.; Barnickel, G.; Bradaczek, H.; Naumann, D.; Rietschel, E.T.; Giesbrecht, P. *J. Bacteriol.*, **1985**, 162, 9.
- [12] Nikaido H. *Microbiol. Mol. Biol. Rev.*, **2003**, 67, 593.
- [13] Snyder, D.S.; McIntosh, T.J. *Biochemistry*, **2000**, 39, 11777.
- [14] Seydel, U.; Koch, M.H.J.; Brandenburg, K. *J. Struct. Biol.*, **1993**, 110, 232.
- [15] Brandenburg, K.; Koch, M.H.J.; Seydel, U. *Eur. J. Biol.*, **1998**, 258, 686.
- [16] Brandenburg, K.; Jürgens, G.; Müller, M.; Fukuoka, S.; Koch, M.H.J. *Biol. Chem.*, **2001**, 382, 1215.
- [17] Jürgens, G.; Müller, M.; Koch, M.H.J.; Brandenburg, K. *Eur. J. Biol.*, **2001**, 268, 4233.
- [18] Brandenburg, K.; Jürgens, G.; Andra, J.; Lindner, B.; Koch, M.H.J.; Blume, A.; Garidel, P. *Eur. J. Biol.*, **2002**, 269, 5972.
- [19] Jürgens, G.; Müller, M.; Garidel, P.; Koch, M.H.J.; Nakakubo, H.; Blume, A.; Brandenburg, K. *J. Endotoxin Res.*, **2002**, 8, 115.
- [20] Brandenburg, K.; Blume, A. *Thermochim. Acta*, **1987**, 119, 127.
- [21] Urbanova, M.; Dukor, R.K.; Pancoska, P.; Gupta, V.P.; Keiderling, T.A. *Biochemistry*, **1991**, 30, 10479.
- [22] Brandenburg, K.; Moriyon, I.; Arraiza, M.D.; Lehwerk-Yvetot, G.; Koch, M.H.J.; Seydel, U. *Thermochim. Acta*, **2002**, 382, 189.
- [23] Buschner, S., *Universität Kiel*, **1999**, Ph.D. thesis.
- [24] Galdiero, F.; Cipollardo de L'Ero, G.; Benedetto, N.; Galdiero, M.; Tufano, M.A. *Infect. Immun.*, **1993**, 61, 155.
- [25] Alurkar, V.; Kamat, R. *Infect. Immun.*, **1997**, 65, 2382.
- [26] Galdiero, M.; D'Isanto, M.; Vitiello, M.; Finamore, E.; Peluso, L. *Microbiology*, **2001**, 147, 2697.
- [27] Galdiero, M.; Vitiello, M.; Sanzari, E.; D'Isanto, M.; Tortora, A.; Longanella, A.; Galdiero, S. *Infect. Immun.*, **2002**, 70, 558.
- [28] Massari, P.; Henneke, P.; Ho, Y.; Latz, E.; Golenbock, D.T.; Wetzler, L.M. *J. Immunol.*, **2002**, 168, 1533.
- [29] Galanos, C.; Lüderitz, O.; Westphal, O. *Eur. J. Bio.*, **1969**, 9, 245.
- [30] Hagge, S.O.; De Cock, H.; Gutschmann, T.; Beckers, F.; Seydel, U.; Wiese, A. *J. Biol. Chem.*, **2002**, 277, 34247.

- [31] Jansen, C.; Wiese, A.; Reubsaet, L.; Dekker, N.; De Cock, H.; Seydel, U.; Tommassen, J. *Biochim. Biophys. Acta*, **2000**, *1464*, 284.
- [32] Kröner, E.E.; Peskar, B.A.; Fischer, H.; Ferber, E. *J. Biol. Chem.*, **1981**, *256*, 3690.
- [33] Cameron, D.G.; Kauppinen, J.K.; Douglas, M.; Mantsch, H.H., *Appl. Spectrosc.*, **1982**, *36*, 245.
- [34] Blume, A.; Garidel, P. in *From Macromolecules to Man*, Kemp Ed.; Elsevier: Amsterdam, **1999**, pp. 109-173.
- [35] Takemura, H.; Kaku, M.; Kohno, S.; Tanaka, H.; Yoshida, R.; Ishida, K.; Mizukane, R.; Koga, H.; Hara, K.; Usui, T.; Ezaki, T. *J. Microbiol. Methods*, **1996**, *25*, 287.
- [36] Gutschmann, T.; Schromm, A.B.; Koch, M.H.J.; Kusumoto, S.; Fukase, K.; Oikawa, M.; Seydel, U.; Brandenburg, K. *Phys. Chem. Chem. Phys.*, **2000**, *2*, 4521.
- [37] Gallati, H. *J. Clin. Chem. Clin. Biochem.*, **1982**, *20*, 907.
- [38] Friberger, P.; Sörskog, L.; Nilsson, K.; Knös, M. in *Detection of Bacterial Endotoxin with the Limulus Amebocyte Lysate Test*, Watson, Levin, and Novitzky. Eds.; A. Liss: New York, **1987**, pp. 149-169.

Received: 01 March, 2005

Accepted: 24 June, 2005